Weak boundary storage liquid crystal displays

K.H. Yang

J. Physique **44** (1983) 1051-1059 SEPTEMBRE **1983**, PAGE 1051

Classification
Physics Abstracts
61.30 — 46.30C — 62.90

Weak boundary storage liquid crystal displays

K. H. Yang

IBM Thomas J. Watson Research Center, P. O. Box 218, Yorktown Heights, NY 10598, USA

(*Reçu le 11 février 1983, révisé le 29 avril, accepté le 5 mai 1983*)

Résumé. — Nous basant sur la théorie d'Oseen et Frank de l'élasticité des cristaux liquides (CL) nématiques et sur une équation d'équilibre des couples à l'interface CL-substrat, nous étudions la déformation statique d'un milieu CL semi-infini, d'une cellule CL homogène et d'une cellule nématique « hélicoïdale » (twisted) en utilisant comme paramètre l'énergie d'ancrage anisotrope LC-substrat (notée C). Des effets de mémoire sont prédits pour une anisotropie d'ancrage suffisamment petite. Nous avons calculé, pour 16 mélanges nématiques disponibles dans le commerce, le domaine de valeur de C pour lequel l'effet de mémoire lié à l'ancrage faible peut se produire dans des cellules homogènes et « hélicoïdales ». Nous avons également trouvé une équation donnant la durée de l'effet de mémoire en fonction de C. Le traitement a été étendu pour rendre compte de la forme la plus générale d'interaction interfaciale CL-substrat. Un tel effet pourrait fournir un moyen de réaliser des dispositifs d'affichage plats, adressés matriciellement, non rafraîchis et de faible puissance.

Abstract. — Based on the Oseen and Frank elastic continuum theory of nematic liquid crystals and on a generalized torque balance equation at the liquid crystal-to-substrate interface, static deformations of a semi-infinite liquid crystal (LC) medium, a homogeneous LC cell, and a twisted nematic cell have been investigated using the anisotropic LC-to-substrate anchoring energy C as a parameter. Storage effects are predicted for sufficiently small anchoring anisotropy. Numerical ranges of C, within which the weak boundary storage effect may occur, have been calculated for sixteen commercially-available nematic LC mixtures in the homogeneous and twisted nematic cell configuration. An equation for the storage time as a function of C has also been derived. The treatment has also been extended to include the most general form of a LC-to-substrate interfacial potential. Such a weak boundary storage effect could provide a means for realizing low power, non-refreshed, matrix-addressed flat panel displays.

1. Introduction.

Conventional direct-view, field-effect liquid crystal displays (LCD), such as twisted nematic (TN) displays and guest-host displays using dichroic dyes as the guest in nematic or cholesteric hosts, have limited multiplex adressing capability [1] because of the high V_{on}/V_{th} ratio, where V_{on} and V_{th} are the root-mean-square voltages for the device to be turned on or at threshold, respectively. Consequently, these LCDs are suitable only for low information content displays such as are found in digital watches. At present, it is too expensive to fabricate these LCDs for displaying information beyond one line of eighty characters. In addition, conventional LCDs have no storage effect, so that direct pel drive or refresh circuits are necessary for their operation. In operating conventional LCDs, voltages larger than the threshold voltage, V_{th}, are applied across the display electrodes to deform the LC medium from its quiescent state. The strain energy induced in the LC medium in the deformed state is generated by two opposing forces-the force due to the electric field and the anisotropic surface anchoring (ASA) force. The magnitude of the strain energy is an increasing function of $\Delta V = V - V_{th}$, where V is the applied voltage. When ΔV decreases, the strain energy decreases accordingly and the LC medium is less deformed. As ΔV approaches zero, the LC medium is restored to its quiescent state.

This paper describes the theoretical investigation of a new class of LCD for which a storage effect is predicted and which has potential application for direct-view, high information content displays. I call this class of displays « weak boundary storage liquid crystal displays (WBSLCDs) » and they are based on the concept of a relatively weak LC-to-substrate anchoring anisotropy which eases the reorientation of the directors of the boundary LC layer by the electric field. The investigation includes calculation of the static deformations of a semi-infinite LC medium, a homo-

geneous LC cell, and a twisted nematic cell, with the anisotropic LC-to-substrate anchoring energy C as a parameter. In all three cases, the current flow, space charge, and mass flow effects in the LC medium are neglected in formulating the free energy of the system. The Oseen [2] and Frank [3] elastic continuum theory of the nematic medium is used to formulate the system free energy. Both the elastic and dielectric anisotropies are considered in obtaining the solutions. While similar calculations with the approximation of equal elastic constants and negligible dielectric anisotropy were carried out by Nehring *et al.* [4] for the cases of homogeneous and twisted nematic cells, the possibility of a weak boundary storage effect was not reported by those authors. In this study, storage effects are predicted for sufficiently small values of C. Numerical results, describing the range of the ASA energy within which the storage effect occurs, are calculated for a number of commercially-available nematic LC mixtures in the homogeneous and TN cell configurations. The storage time as a function of the ASA energy is derived and illustrated numerically for the nematic mixture E7 (British Drug House).

2. Semi-infinite LC medium.

We consider the case of a nematic LC medium of positive dielectric anisotropy in contact with a wall at $z = 0$ and extending to infinity along the $+ z$ axis. The LC layer in contact with the wall is anisotropically anchored with LC directors parallel to each other and to the wall. If a uniform electric field E is applied to the LC medium along the $+ z$ axis, the relative free energy per unit area in the xy-plane can be written as :

$$F \equiv \int_0^d f(z)\, dz \tag{1}$$

with d approaching ∞. The function $f(z)$ can be expressed as :

$$f(z) = \frac{1}{2}(k_{11}\cos^2\theta + k_{33}\sin^2\theta)\left(\frac{d\theta(z)}{dz}\right)^2 + \frac{1}{2}\frac{D_\infty^2}{\varepsilon_\parallel \sin^2\theta(z) + \varepsilon_\perp \cos^2\theta(z)} - \frac{1}{2}C\delta(z)\cos^2\theta(z), \tag{2}$$

where $\theta(z)$ is the angle between the LC directors at position z and the wall surface; k_{11}, k_{33}, $\varepsilon_\parallel$, and $\varepsilon_\perp$ are the LC elastic splay and bend constants, and the dielectric permittivity parallel to and perpendicular to the LC directors, respectively. C is the anisotropic LC-to-substrate anchoring energy per unit area and is always positive in this paper. D_∞ is the dielectric displacement at $z = \infty$. $\delta(z)$ is the Dirac delta function. The last term in (2) describes the interfacial ASA energy per unit area as a function of θ. It assumes the existence of a surface order parameter similar to the bulk order parameter of Maier-Saupe [5].

The boundary condition due to the balance of torque at $z = 0$ is

$$(k_{11}\cos^2\theta_0 + k_{33}\sin^2\theta_0)\left(\frac{d\theta}{dz}\right)_{z=0} - C\sin\theta_0\cos\theta_0 = 0 \tag{3}$$

where θ_0 is $\theta(z)$ evaluated at $z = 0$.

After applying the calculus of variations to minimize the system free energy associated with equations 1 and 2 and integrating once, we get

$$(k_{11}\cos^2\theta + k_{33}\sin^2\theta)\left(\frac{d\theta}{dz}\right)^2 = \frac{D_\infty^2}{\varepsilon_\parallel^2}\varepsilon_a\frac{\cos^2\theta}{(1 - \alpha\cos^2\theta)} \tag{4}$$

where $\varepsilon_a \equiv \varepsilon_\parallel - \varepsilon_\perp$ and $\alpha \equiv \varepsilon_a/\varepsilon_\parallel$. Equation 3 becomes

$$\frac{D_\infty}{\varepsilon_\parallel}\sqrt{\varepsilon_a k_{33}}\sqrt{\frac{1 - \gamma_1\cos^2\theta_0}{1 - \alpha\cos^2\theta_0}}\cos\theta_0 = C\cos\theta_0\sin\theta_0, \tag{5}$$

where $\gamma_1 \equiv (k_{33} - k_{11})/k_{33}$.

The solutions of (5) are

$$\cos\theta_0 = 0 \rightarrow \theta_0 = \frac{\pi}{2} \tag{6}$$

and

$$\sin^2\theta_0 = \eta^2\left(\frac{1 - \gamma_1\cos^2\theta_0}{1 - \alpha\cos^2\theta_0}\right), \tag{7}$$

where

$$\eta \equiv \frac{D_\infty}{\varepsilon_\parallel C}\sqrt{\varepsilon_a k_{33}}. \tag{8}$$

Figure 1 shows the result of the calculation using (7) and (8) with E7 as the LC material. In this figure, E_c is defined as $E_c = C/\sqrt{\varepsilon_a k_{33}}$ and $E = D_\infty/\varepsilon_\parallel$. E_c is the

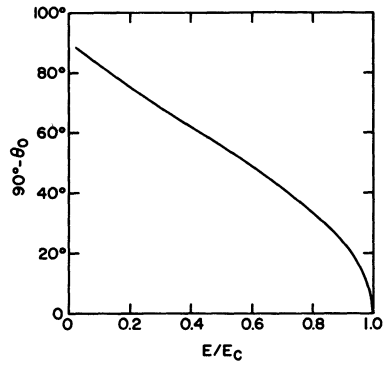

Fig. 1. — The tilt angle of the boundary LC layer as a function of the applied electric field as calculated using liquid crystal E7 in the configuration of a semi-infinite medium.

critical electric field above which the directors of the LC medium including the boundary layer are aligned parallel to the z axis. Since $C > 0$, consideration of the system free energy excludes the solution of (6) ($\theta_0 = \pi/2$) unless $\eta \geqslant 1$.

3. Homogeneous LC cell.

Consider a nematic layer of thickness d confined between the planes $z = 0$ and $z = d$. The LC directors always lie in the xz-plane and, in the absence of an external electric field, the directors are everywhere parallel to the x axis. The tilt angle between the director at position z and the x axis is denoted by $\theta(z)$. If the ASA force is the same for both cell substrates, the solutions of the problem are symmetrical with respect to the $z = d/2$ plane. In the following, symbols with subscript 0 and m denote the corresponding functional values evaluated at $z = 0$ and $z = d/2$, respectively. The system free energy per unit area is described by (1) with d retaining a finite value. The function $f(z)$ now becomes the following :

$$f(z) = \frac{1}{2}(k_{11}\cos^2\theta + k_{33}\sin^2\theta)\left(\frac{d\theta}{dz}\right)^2 + \frac{1}{2}\frac{D_m^2}{\varepsilon_{\|}} \times \frac{1}{(1 - \alpha\cos^2\theta)} - \frac{C}{2}[\cos^2\theta.\delta(z) + \cos^2\theta.\delta(z - d)], \quad (9)$$

where D_m is the dielectric displacement at $z = d/2$. The boundary condition is formulated as

$$(k_{11}\cos^2\theta_0 + k_{33}\sin^2\theta_0)\left(\frac{d\theta}{dz}\right)_0 - C\cos\theta_0\sin\theta_0 = 0. \quad (10)$$

Applying the calculus of variations to minimize the system free energy associated with equations 1 and 9 and after some manipulation, we have for $V \geqslant V_{th}$

$$v \equiv \frac{V}{U} = \frac{2}{\pi}\sqrt{1 - \alpha\cos^2\theta_m} \times \int_{\theta_0}^{\theta_m}\left\{\frac{1 - \gamma_1\cos^2\theta}{(1 - \alpha\cos^2\theta)[\cos^2\theta - \cos^2\theta_m]}\right\}^{1/2} d\theta, \quad (11)$$

with

$$U \equiv \pi(k_{33}/\varepsilon_a)^{1/2}, \quad (11a)$$

where V is the applied voltage across the cell and V_{th} is the threshold voltage for a Freedericksz transition of the LC cell. Equation 10 becomes

$$\sin^2\theta_0\cos^2\theta_0 = (1 - \gamma_1\cos^2\theta_0)\,\eta^2 \times \frac{(\cos^2\theta_0 - \cos^2\theta_m)}{(1 - \alpha\cos^2\theta_m)(1 - \alpha\cos^2\theta_0)}, \quad (12)$$

where

$$\eta^2 \equiv \frac{D_m^2}{\varepsilon_{\|}^2}\frac{\varepsilon_a k_{33}}{C^2}. \quad (13)$$

The formulas to evaluate the threshold voltage and the saturation voltage can be derived using (11) and (12) in the limits of $\theta_0 \to \theta_m \to 0$ and $\theta_0 \to \theta_m \to \pi/2$.

The results are

$$\operatorname{cotg}\left[\frac{\pi}{2}\frac{v'}{(1 - \gamma_1)^{1/2}}\right] = \lambda v'(1 - \gamma_1)^{1/2} \quad (14)$$

and

$$\operatorname{cotgh}\left[\tfrac{1}{2}\pi v''\right] = \lambda v'', \quad (15)$$

where $v' \equiv V_{th}/U$, $v'' \equiv$ saturation voltage (corresponds to $\theta_m = \theta_0 = \pi/2)/U$ and

$$\lambda \equiv \frac{\pi k_{33}}{Cd}. \quad (16)$$

In the limit of $k_{11} = k_{22} = k_{33}$, equations 14 and 15 reduce to those derived by Nehring *et al.* [4]. Using E7 as a LC material, the calculated values of v'' and v' as a function of λ are shown in figure 2. In the limit $C \to \infty$ ($\lambda \to 0$), v'' goes to infinity. In the case of a vanishing ASA force, $v'' = v'$ goes to zero. As indicated in figure 2, v'' approaches v' as C becomes sufficiently small, for fixed d.

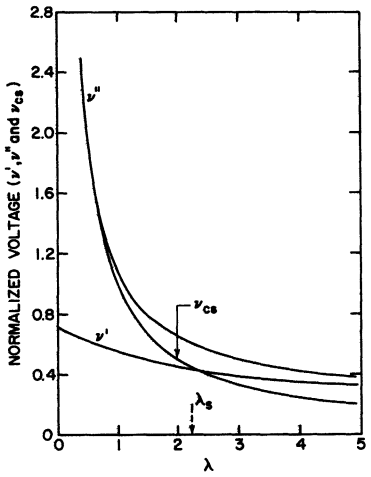

Fig. 2. — Numerical results for v' (threshold voltage), v'' (saturation voltage) and v_{cs} as a function of $\lambda = \pi k_{33}/Cd$. The nematic mixture E7 is assumed for the calculation.

The weak boundary storage effect occurs when C becomes small enough (for example $\lambda = 2.3$ in Fig. 2). We drive the LC cell to saturation by the electric field so that $\theta_m = \theta_0 = \pi/2$. The applied voltage is then lowered to a value smaller than the saturation voltage. Equation 12 implies that, as $\theta_m = \pi/2$, the solution for θ_0 (using E7 as an example) is equal to $\pi/2$ as long as

$\eta \geqslant 1$. In the case of $\eta < 1$, equation 12 reduces to (7) and (6) if $\theta_m = \pi/2$. From (13), $\eta = 1$ implies

$$v_{cs} \equiv \frac{V_{cs}}{U} = \frac{dC}{\pi k_{33}} = \frac{1}{\lambda}, \tag{17}$$

where V_{cs} is equal to $d \times E_c$ (see section 2) above which the saturation state ($\theta_m = \theta_0 = \pi/2$) of the LC cell is maintained. Equation 17 is also plotted in figure 2 for comparison. In figure 2, we can see that the v_{cs} and v' curves intersect at $\lambda = \lambda_s = 2.30$. When $\lambda > \lambda_s$, and a line-at-a-time, three-to-one multiplex addressing scheme is used, the unaddressed LC pels remain quiescent if the bias voltage is equal to or less than V_{th} while the selected LC pels can be driven to the saturation state and remain in that state, constituting the storage effect. From equations 15 and 17 and figure 2, we can see that v_{cs} is always less than v''. The saturation voltage is the applied voltage which is necessary to overcome the ASA force and the LC long range ordering force confined by a cell of spacing d. After saturation, the LC long range ordering force cooperates with the applied electric field against the ASA force. This is the fundamental mechanism that leads to the storage effect.

Given λ, if the bias voltage is at $V = vU$ after a homogeneous cell is driven into saturation, the storage time as a function of v can be expressed [6] as

$$\tau(\lambda) = \frac{\tau_0}{[v'(\lambda)/v'(0)]^2} \cdot \frac{1}{\left[1 - \left(\frac{v}{v_{cs}(\lambda)}\right)^2\right]} \quad \text{if} \quad v \leqslant v_{cs}(\lambda) \tag{18}$$

$$= \infty \quad \text{if} \quad v > v_{cs}(\lambda),$$

where τ_0 is equal to $\rho d^2/\pi^2 k_{33}$ and ρ is the viscosity of the LC medium. The criterion to achieve an infinite storage time is

$$v \geqslant v_{cs}(\lambda). \tag{19}$$

If the bias voltage is the same as the threshold voltage, i.e. $v = v'(\lambda)$, equation 19 with an equal sign has a solution at $\lambda = \lambda_s$ as shown in figure 2. In this case, the electric field associated with v_{cs} at $\lambda = \lambda_s$ corresponds to E_c in the case of a semi-infinite LC medium (see section 2). We define λ_{31} as the value above which a line-at-a-time, three-to-one multiplex address scheme has the capability of driving the selected LC pel to saturation when the bias voltage for the unselected pels is at V_{th}. Table I lists LC mixtures and their physical constants as used for the calculation. The calculated values of λ_{31} and λ_s for sixteen nematic LC mixtures are listed in table II. The ASA energy per unit area for the storage condition to occur can be calculated using (14), (17), and (19) once the cell spacing is chosen. Infinite storage time occurs for those cells satisfying the condition that $\lambda \geqslant \lambda_s$ with any multiplex address scheme which has the capability of driving the selected pels into saturation and biases those pels and the unselected pels at $V = V_{th}$. The solid curve in figure 3 shows the storage time as a function of λ using E7 as nematic LC and (18) with $v = v'(\lambda)$.

Table I.

LC Mixtures	k_{11} (10^{-7} dynes)	k_{22} (10^{-7} dynes)	k_{33} (10^{-7} dynes)	T_{NI} (°C)	Reference
TN200	8.8	8.35	19.0	65.5	15
TN201	13.03	13.30	25.4	104.8	15
TN211	11.10	10.20	17.6	76.3	15
TN103	11.4	7.30	18.6	81.4	15
TN132	9.7	7.8	15.9	60.7	15
TN403	12.6	10.8	23.10	82.1	15
TN430	10.7	9.10	18.30	69.2	15
E7	10.7	10.0	20.7	59	15
ZLI1132	8.7	9.0	21.0	71	15
TN621	12.0	6.72	16.9	76.5	16
TN605	12.1	6.78	19.8	96	16
TN623	14.7	7.06	19.4	101	16
TN701	9.0	5.4	14.4	62.5	16
TN615	10.0	5.25	13.9	70.5	16
TN619	11.1	5.22	10.9	60.5	16
TN703	9.6	5.47	14.6	68.5	16

Table II. — *Homogeneous cell.*

LC Mixtures	λ_{31}	λ_s	C_{31} (10^{-3} ergs/cm^2)	C_s (10^{-3} ergs/cm^2)
TN200	0.58	2.36	10.30	2.53
TN201	0.55	2.30	14.51	3.47
TN211	0.50	2.20	11.06	2.51
TN103	0.51	2.20	11.46	2.66
TN132	0.51	2.20	9.79	2.27
TN403	0.53	2.29	13.69	3.17
TN430	0.52	2.24	11.06	2.57
E7	0.55	2.30	11.82	2.82
ZLI1132	0.61	2.45	10.81	2.69
TN621	0.49	2.14	10.84	2.48
TN605	0.49	2.21	12.69	2.81
TN623	0.48	2.10	12.70	2.90
TN701	0.51	2.20	8.87	2.06
TN615	0.49	2.10	8.91	2.08
TN619	0.42	2.00	8.22	1.73
TN703	0.50	2.18	9.17	2.10

4. Twisted nematic cell.

We now consider the twisted nematic LC cell with a cell spacing d and the z-axis normal to the cell substrates. Two angles are now required to specify the deformation of the LC directors in space : a tilt angle θ which, as before, specifies the angle between the LC director and the xy-plane and an azimuthal twist

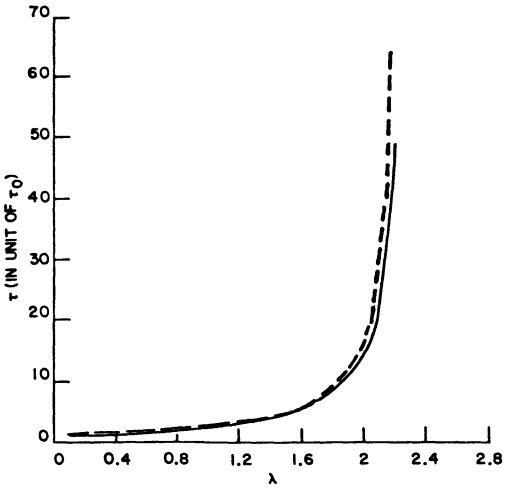

Fig. 3. — The solid curve denotes the storage time as a function of λ using E7 in the configuration of a homogeneous cell according to equation 18 with $v = v'(\lambda)$. The dashed curve is the corresponding result for a TN cell.

angle ζ corresponding to the orientation of the projection of the director on the xy-plane with respect to the x-axis. For convenience, we specify $\zeta(d/2) = 0$. Symbols with subscripts 0 and m denote the corresponding functional values evaluated at $z = 0$ and $d/2$, respectively.

The free energy of the system per unit area is expressed by equation 1 with d retaining a finite value. The function $f(z)$ can be written as :

$$f(z) = \frac{1}{2}k_{33}(1 - \gamma_1 \cos^2\theta)\left(\frac{d\theta}{dz}\right)^2 + \frac{1}{2}k_{33}(1 - \gamma_2 \cos^2\theta)\cos^2\theta\left(\frac{d\zeta}{dz}\right)^2 + \frac{1}{2}\frac{D_m^2}{\varepsilon_{\parallel}}\frac{1}{(1-\alpha\cos^2\theta)} - \frac{1}{2}C\cos^2\theta[\delta(z)+\delta(z-d)], \tag{20}$$

where $\gamma_2 \equiv (k_{33} - k_{22})/k_{33}$ and k_{22} is the twist elastic constant of the LC medium. The dependence of the anisotropic interfacial potential on ζ is neglected by assuming that the director of the boundary LC layer moves mainly in θ rather in ζ. Again, applying the calculus of variations to minimize the system free energy associated with (1) and (20), and performing the integration once, we have

$$(1 - \gamma_1 \cos^2\theta)\left(\frac{d\theta}{dz}\right)^2 + (1 - \gamma_2 \cos^2\theta)\cos^2\theta\left(\frac{d\zeta}{dz}\right)^2 - \frac{D_m^2}{\varepsilon_{\parallel} k_{33}}\frac{1}{(1 - \alpha\cos^2\theta)} = a^2, \tag{21}$$

with

$$a^2 = \frac{b^2}{(1 - \gamma_2 \cos^2\theta_m)\cos^2\theta_m} - \frac{D_m^2}{\varepsilon_{\parallel} k_{33}}\frac{1}{(1 - \alpha\cos^2\theta_m)} \tag{21a}$$

and

$$(1 - \gamma_2 \cos^2\theta)\cos^2\theta\frac{d\zeta}{dz} = b, \tag{22}$$

where a and b are constants of integration. Again, we have assumed the symmetrical properties of the cell with respect to the $z = d/2$ plane so that $(d\theta/dz)_m = 0$.

If parallel grooves on the substrates (such as are generated by rubbing) are used to align the boundary LC layer, the director of the boundary LC layer tends to change in θ rather than in ζ when the applied voltage exceeds the threshold voltage. In this case, the boundary condition due to the balance of torque at $z = 0$ is

$$k_{33}(1 - \gamma_1 \cos^2\theta_0)\left(\frac{d\theta}{dz}\right)_0 - C\cos\theta_0 \sin\theta_0 = 0. \tag{23}$$

Substituting (21) and (22) into (23), we have

$$\sin^2\theta_0 \cos^2\theta_0 = \left[\frac{k_{33}^2 b^2}{C^2}\cdot\frac{(1 - \gamma_2(\cos^2\theta_0 + \cos^2\theta_m))}{(1 - \gamma_2\cos^2\theta_0)(1 - \gamma_2\cos^2\theta_m)\cos^2\theta_0\cos^2\theta_m} + \frac{\eta^2}{(1 - \alpha\cos^2\theta_0)(1 - \alpha\cos^2\theta_m)}\right] \times (1 - \gamma_1\cos^2\theta_0)(\cos^2\theta_0 - \cos^2\theta_m), \tag{24}$$

where η is specified by equation 13. Below the threshold voltage for a Freedericksz transition of the LC cell, it can be shown from (22) that

$$b = (1 - \gamma_2)(\phi_T/d), \tag{25}$$

where ϕ_T specifies the angle of the initial twist. Using (21) to (25) and taking the limit $\theta_0 \to \theta_m \to 0$ as in the case of the homogeneous cell, we obtain [7] the following equation :

$$\operatorname{cotg}\left(\frac{1}{2}\frac{((1-2\gamma_2)\phi_T^2+\pi^2 v'^2)^{1/2}}{(1-\gamma_1)^{1/2}}\right)=\frac{\lambda}{\pi}\times((1-2\gamma_2)\phi_T^2+\pi^2 v'^2)^{1/2}\times(1-\gamma_1)^{1/2} \tag{26}$$

where $v' \equiv V_{th}/U$ and λ and U are as defined in section 3. In the case of infinite ASA force ($\lambda \to 0$), equation 26 implies that

$$V_{th}=\frac{1}{\sqrt{\varepsilon_a}}(k_{11}\pi^2+(k_{33}-2k_{22})\phi_T^2)^{1/2}, \tag{27}$$

which is the same as derived by Leslie [8]. If we assume $k_{11}=k_{22}=k_{33}=k$, equation 26 reduces to the result reported by Nehring *et al.* [4]. In the limit $\phi_T = 0$, equation 26 reduces to equation 14, as it should.

Equation 22, with a non-zero constant b, is not relevant to describe the saturation condition. Since at saturation, according to (22), cos θ goes to zero as θ approaches $\pi/2$, $d\zeta/dz$ diverges for all z unless b is equal to zero. Therefore, at saturation, b should approach zero as $\theta_0 \to \pi/2$. In order to satisfy the condition of saturation and to be compatible with equation 26 and 15 for the case $\phi_T = 0$, I make the following assumption :

$$\lim_{\theta_0\to\pi/2}\frac{b^2}{\cos^2\theta_0\cos^2\theta_m}=(1-2\gamma_2)\left(\frac{\phi_T}{d}\right)^2. \tag{28}$$

Using (21), (22), (23), (24), and (28) and taking the limit that $\theta_0 \to \theta_m \to \pi/2$, we derive the following equation to describe the saturation voltage as a function of λ :

$$\operatorname{cotgh}\left(\frac{1}{2}\sqrt{(1-2\gamma_2)\phi_T^2+\pi^2 v''^2}\right)=\frac{\lambda}{\pi}\sqrt{(1-2\gamma_2)\phi_T^2+\pi^2 v''^2}, \tag{29}$$

with $v'' \equiv$ saturation voltage/U.

In the case that $\phi_T = 0$, (29) is the same as (15). If we assume $k_{11}=k_{22}=k_{33}$, (29) reduces to

$$\operatorname{cotgh}\left(\frac{1}{2}\sqrt{\phi_T^2+\pi^2 v''^2}\right)=\frac{\lambda}{\pi}\sqrt{\phi_T^2+\pi^2 v''^2}, \tag{30}$$

which is slightly different from the following equation, derived by Nehring *et al.* [4]

$$\lambda v''\left[\tan^2\left(\frac{1}{2}\phi_T\right)+\tanh^2\left(\frac{1}{2}\pi v''\right)\right]=\left(1+\tan^2\left(\frac{1}{2}\phi_T\right)\right)\tanh\left[\frac{1}{2}\pi v''\right]. \tag{31}$$

Equation 31 predicts that, for $\phi_T = \pi/2$, v'' decreases to zero at $\lambda = \pi$ as compared to $\lambda = 3.05$ using (30). The numerical solutions for v'' as a function of λ using (30) and (31) are shown in figure 4 for comparison. The difference is very small. From (31), we can also generate the solution for the case of unequal elastic constants. The replacement of ϕ_T with $(1-2\gamma^2)^{1/2}\phi_T$ in (31) will result in an equation which is compatible with (26) and (15) in the limit $\phi_T = 0$. The numerical difference in v'' calculated from this generalized equation and (29) is smaller than that shown in figure 4 for the sixteen nematic mixtures listed in table I.

The solution for v' and v'' as a function of λ from (26) and (29) (or an equation generalized from equation 31) depends on the sign of $(1-2\gamma_2) = 2k_{22}-k_{33}$. If $(1-2\gamma_2)$ is negative, as for E7, both v' and v'' asymptotically approach $\phi_T\sqrt{(2\gamma_2-1)}/\pi$ as λ approaches infinity. In the case that $(1-2\gamma_2)$ is positive, as for TN211, both v' and v'' decrease to

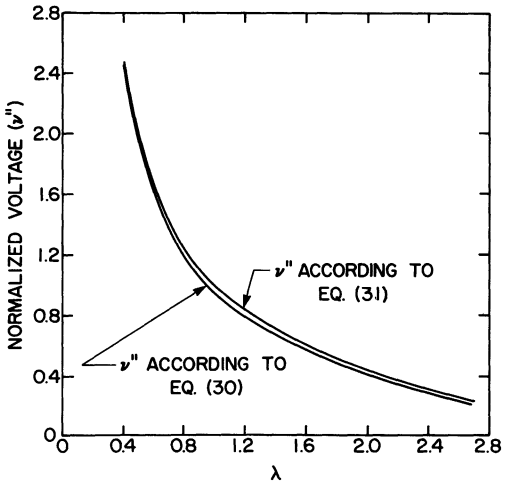

Fig. 4. — The solid curves denote the saturation voltage v'' as a function of λ in the case of equal elastic constants and a $\pi/2$-twist cell, using equation 30 and the equation derived by Nehring *et al.* in reference 4 (or Eq. 31 in this paper).

zero at finite values of λ. The numerical values of v' and v'' as a function of λ are calculated and shown in figure 5 for E7 and in figure 6 for TN211. These figures show the physical significance of the sign of $(1 - 2\gamma_2)$. When it is negative, the uniform twisted structure is stable for all values of λ in the absence of the external field. When it is positive, with no applied field, the uniform twisted structure is stable as long as $\lambda \leqslant \lambda'$ (in Fig. 6). As the ASA force is reduced, the alignment becomes spontaneously tilted for values of λ in the range $\lambda' < \lambda < \lambda''$ (Fig. 6). With further weakening of the ASA force, the twisted cell is not stable and a homeotropic alignment should occur for $\lambda > \lambda''$.

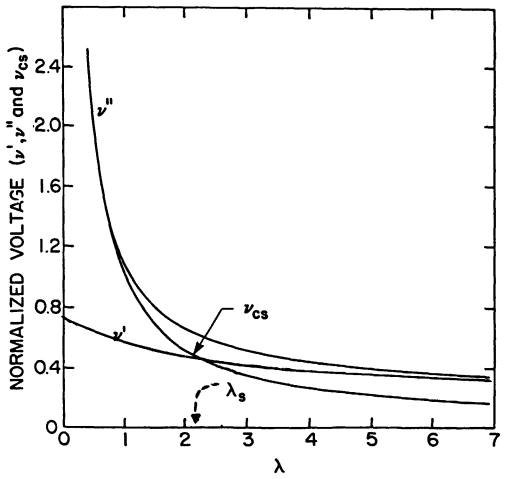

Fig. 5. — Numerical results for v', v'' and v_{cs} as a function of λ using E7 in a $\pi/2$-twisted nematic configuration. In this case $(1 - 2\gamma_2)$ is negative.

From these figures, we can see that as the ASA force is weakened, v''/v' is reduced so that the multiplex capability of the TN cell is improved. However, the WBS effect will occur in the TN cell also when the ASA force is sufficiently weak. Given the λ value, we can drive the TN cell into saturation and then lower the applied voltage corresponding to v. It can be shown from equation 24 that the saturation state remains if

$$v \geqslant v_{cs} \equiv \frac{1}{\lambda}[1 - \phi_T^2(1 - 2\gamma_2)/\pi^2]^{1/2}. \quad (32)$$

In (32), the term containing ϕ_T, denoting the effect due to the twist of a TN cell, is much smaller than unity for the sixteen LC mixtures listed in table I. The curve $v_{cs} = \frac{1}{\lambda}\left(1 - \frac{\phi_T^2}{\pi^2}(1 - 2\gamma_2)\right)^{1/2}$ is plotted in figures 5 and 6 for comparison. I have calculated λ_{31} and λ_s for each of the LC mixtures in a TN cell. The physical meanings of these parameters are defined in the previous section. Figure 5 shows that infinite storage time should occur in an E7 $\pi/2$-

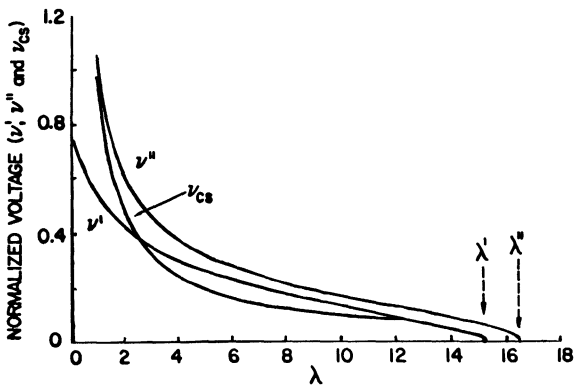

Fig. 6. — Numerical results for v', v'' and v_{cs} as a function of λ using the nematic mixture TN211 in a $\pi/2$-twisted nematic configuration. In this case $(1 - 2\gamma_2)$ is positive so that v' and v'' go to zero at finite values of λ.

twist cell if we can properly prepare the substrates of the LC cell such that $\lambda_s \geqslant 2.23$ and use a line-at-a-time, three-to-one multiplex address scheme. The calculation also shows that, in a TN211 $\pi/2$-twist cell, a similar WBS effect will appear if $12.3 \geqslant \lambda \geqslant 2.58$. The upper limit of $\lambda = 12.3$ is due to the rapidly diminishing v' because of the positive sign of $(1 - 2\gamma_2)$. TN211 was used here to illustrate the qualitative behaviour of positive-$(1 - 2\gamma_2)$ material. The numerical results for λ_{31} and λ_s are tabulated in table III for sixteen LC mixtures

Table III. — *TN cell.*

LC Mixtures	λ_{31}	λ_s	C_{31} (10^{-3}ergs/cm^2)	C_s (10^{-3}ergs/cm^2)
TN200	0.55	2.13	10.86	2.80
TN201	0.56	2.43	14.25	3.28
TN211	0.69	2.58	8.01	2.14
TN103	0.49	1.88	11.93	3.11
TN132	0.51	2.18	9.79	2.30
TN403	0.53	2.15	13.69	3.38
TN430	0.52	2.22	11.06	2.59
E7	0.55	2.23	11.82	2.91
ZLI1132	0.58	2.14	11.38	3.08
TN621	0.46	1.84	11.54	2.89
TN605	0.47	1.79	13.24	3.47
TN623	0.44	1.76	13.85	3.46
TN701	0.48	1.84	9.42	2.45
TN615	0.46	1.80	9.49	2.42
TN619	0.43	1.91	8.03	1.81
TN703	0.47	1.82	9.76	2.52

with $\pi/2$-twist configuration. The storage time of a TN cell satisfies an equation similar to (18). The numerical results for storage time as a function of λ using E7 in a TN cell and $v = v'(\lambda)$ are shown in figure 3 as the dashed curve. Infinite storage time occurs at $\lambda \geqslant 2.23$.

5. Discussion and conclusions.

The use of (28) to simplify the computation only affects λ_{31} in table III. Although the exact solution for v'' of TN cells is not obtained, its influence on the storage effect is believed to be minor. This is the subject of further research.

Using λ_s in tables II and III and equation 16 we can calculate the upper limit of the ASA energy per unit area, C, for each nematic LC. Below this upper limit, a line-at-a-time, three-to-one or two-to-one multiplex address scheme can drive the selected LC pels into saturation and keep them in that state under the low, constant bias field. The stored saturation state is erasable if the bias field vanishes or is reduced to a small value for a sufficiently long period of time. The force associated with the ASA energy per unit area is responsible for the erasability. Assuming $d = 10$ μm, the calculated values of C_{31} and C_s corresponding to λ_{31} and λ_s are listed in tables II and III for sixteen nematic LC mixtures in the homogeneous and TN cell configurations, respectively. The data in tables II and III imply that, if C is in the region of 0.002 ergs/cm^2, the WBS effect should occur. According to (16), given λ, the value of C_s is inversely proportional to d so that a thinner LC cell implies a larger value of C_s.

As pointed out by Nehring *et al.*, weakening the ASA force will shorten the display rise time but lengthen the display turn-off time. The calculation of the rise time under the weak ASA condition is beyond the scope of this paper. The turn-off time is estimated by Nehring *et al.* [4] and can be expressed as $\tau_0\left[\frac{v'(\lambda)}{v'(0)}\right]^2$ where τ_0 is the turn-off time corresponding to the infinite ASA condition. If $\lambda = 1$, the turn-off time is equal to 2.5 τ_0 which is in the region of 100 ms. The turn-off time is equivalent to the erase time when the storage effect is utilized. In addition, because the on state corresponds to the saturation state, the angular appearance of a WBS TN cell should be improved.

From this analysis, the important parameter for the WBS effect to occur is C, the ASA energy per unit area. Some remarks on the experimental determination of C are relevant. Rapini and Papoular [9] estimated that C is approximately 1 erg/cm^2. Ryschenkow and Kleman [10] followed the analysis of Vitek and Kleman [11] and derived an approximate equation for the energy associated with disclination lines. Assuming equal elastic constants, they obtained a value of 10^{-4} ergs/cm^2 for C. To anchor the 4-methoxybenzylidene-4'-n-butylaniline (MBBA) LC, Rychenkow and Kleman evaporated the product of degradation from heated paper at a temperature of 400 °C for a few minutes until the smoke deposited a brown film on the interior surface of the glass plate. Riviere *et al.* [12] utilized obliquely evaporated SiO to anchor the nematic LC 6CB (4-cyano-4'-n-hexylbiphenyl) in a wedged cell. They used the Oseen and Frank elastic continuum theory with the assumption of equal elastic constants to analyse the orientation of LC directors in the cell. The method of attenuated total reflection was used to measure the tilt angle of the LC layer adjacent to the substrate. They determined a value of $(4.2 \pm 1.6) \times 10^{-3}$ ergs/cm^2 for C. Naemura [13] measured the Freedericksz threshold field of a homeotropically aligned MBBA cell in a magnetic field with the cell spacing as a parameter to determine the ASA energy. The C values ranged from 1.0×10^{-2} ergs/cm^2 with surfactant FS 150 [13] as the anchoring agent on indium oxide coated glass to 2.6×10^{-3} ergs/cm^2 with hexadecyl amine as the anchoring agent on bare glass. Scheffer [14] utilized a glass hemisphere and a flat glass plate with the nematic LC TN403 filled in between. Monochromatic parallel light was passed through the hemisphere to generate Newton rings. The LC medium was homogeneously aligned on the flat glass plate by oblique evaporation of SiO and homeotropically aligned on the hemisphere by DMOAP [14] treatment. The observation of Newton rings as a function of spacing led him to determine the effective index of refraction, which is related to the orientation of the LC directors. The Oseen and Frank elastic continuum theory was used to calculate the orientation of the LC director as a function of position taking into account the elastic anisotropy and the boundary conditions. Based upon the effective index of refraction associated with the Newton rings, he determined $C \geqslant 0.1$ ergs/cm^2 for both the surfactants and evaporated-SiO alignments.

The reproducibility of Ryschenkow and Kleman's method of alignment is questionable and the approximate equation describing the energy of surface disclination lines with the assumption of equal elastic constants precludes an estimation of possible experimental errors. The result of Riviere *et al.* is probably valid to within a factor three because of the assumption of equal elastic constants. The results of Naemura and Scheffer are probably more reliable. However, since the above authors differ in choosing either the LC materials, or the anchoring methods on properly prepared substrates, it is difficult to draw any conclusions based on a comparison of their results.

In this paper as well as in the analysis of the above experimental results, a LC-to-substrate interfacial potential of $-0.5 \times C \cos^2\theta$ has been assumed. In a general case, because of the inversion symmetry of the nematic LC, the LC-to-substrate interfacial potential $I(\theta)$ can be expressed as :

$$I(\theta) = \sum_{n=1}^{\infty} A_{2n} \times P_{2n}(\cos\theta) = \text{const.} - 0.5 \times C \cos^2\theta - 0.5 \times \left[\sum_{n=2}^{\infty} C_{2n} \cos^{2n}\theta\right], \quad (33)$$

where $P_{2n}(\cos\theta)$ are the Legendre polynomials and

C, C_{2n}, and A_{2n} are constants. Using the generalized interfacial potential, equations 14 and 26 are still valid for the calculation of threshold voltages of a homogeneous cell and a TN cell, respectively. However, the parameter λ in these two equations should be changed to the form :

$$\lambda \equiv \pi \times k_{33}/(d \times G), \tag{34}$$

where $G \equiv C + 2\,C_4 + 3\,C_6 + \cdots + nC_{2n} + \cdots$. The equations for calculating v_{cs} and the saturation voltages of a homogeneous cell and a TN cell remain the same (i.e., $\lambda = \pi k_{33}/(dC)$) as described in sections 3 and 4. We can see that, if higher-order terms than $\cos^2\theta$ are included in the interfacial potential, the value of C can be determined from experiments performed near the region of the saturation voltage. According to equations 33 and 34, at the threshold voltage, the anchoring anisotropy is characterized by G instead of C. The anchoring anisotropy deduced from experiments performed near the threshold voltage, such as those of Naemura and Riviere *et al.*, should be equal to G instead of C. Hence, it is possible that the anchoring anisotropy may appear stronger near the saturation voltage if C is large while it may appear weaker near the threshold voltage if G is small. Our preliminary experimental results [17] seem to indicate that the interfacial potential is of the form $-0.5 \times (C\cos^2\theta + C_4\cos^4\theta)$ where C is positive but C_4 is negative. As an example, if $C = 10^{-2}$ ergs/cm^2 $> (G = C + 2\,C_4 = 0.002$ ergs/cm^2), the WBS effect could probably be observed only under the condition of extremely thin cell spacing [17]. Extremely thin cells are being fabricated for the verification of the WBS effect.

Following my analysis in this paper and taking into account the generalized interfacial potential, it can be shown that the WBS effect exists in a homogeneous cell as well as in a TN cell with a negative-$(1 - 2\,\gamma_2)$ LC medium. It would be possible to observe the WBS effect if both C and G were small and in the region of 0.002 ergs/cm^2 for a 10 μm cell. On the other hand, if the anchoring anisotropy is weak at the threshold voltage and strong at the saturation voltage or *vice versa*, the WBS effect could probably be observed only under the condition of extremely thin cell-spacing. In this case, the application of the WBS effect for display devices would be difficult to realize.

Based on the Oseen and Frank elastic continuum theory of the nematic LC, I have analysed the conditions under which a storage effect will take place for homogeneous and TN cells. Below the saturation voltage, the applied electric field acts against both the ASA force and the LC long-range ordering force in order to distort the LC medium. After driving the LC cell to saturation, the ASA force opposes the applied electric field and the LC long-range ordering force for the restoration of the LC medium to its quiescent state. If the ASA force is sufficiently weak, a storage effect occurs when the applied voltage, after exceeding the saturation voltage for a sufficiently long period of time, is reduced to a value less than the saturation value but greater than $d \times E_c$. The storage mechanism has potential application in high-information-content non-refreshed flat panel displays.

Acknowledgments.

The author acknowledges several useful discussions with Dr. W. E. Howard.

References

[1] Alt, P. M. and Pleshko, P., *IEEE Trans. Elec. Dev.* **ED-21** (1973) 990.

[2] Oseen, C. W., *Trans. Faraday Soc. Disc.* **29** (1933) 883.

[3] Frank, F. C., *Faraday Soc. Disc.* **25** (1958) 19.

[4] Nehring, J., Kmetz, A. R. and Scheffer, T. J., *J. App. Phys.* **47** (1976) 850.

[5] Maier, W. and Saupe, A., *Z. Naturforschg* **14a** (1959) 882 and **15a** (1960) 287.

[6] In the approximation of equal elastic constant k, the dynamical equation describing the LC orientation neglecting flow effects can be written as $\varepsilon_a E^2 \sin\phi \times \cos\phi + k\frac{d^2\phi}{dz^2} - \rho\frac{d\phi}{dt} = 0$ where ρ is the viscosity of the LC medium. In the saturation state, ϕ is small so that $\sin\phi \cong \phi$. We obtain equation 18 by Fourier transform.

[7] Yang, K. H., IBM RC report 9852 (Feb., 1983) (submitted to *Appl. Phys. Lett.*).

[8] Leslie, F. M., *Mol. Cryst. Liq. Cryst.* **12** (1970) 57.

[9] Rapini, A. and Papoular, M., *J. Physique Colloq.* **30** (1969) C4-54.

[10] Ryschenkow, G. and Kleman, M., *J. Chem. Phys.* **64** (1976) 404.

[11] Vitek, V. and Kleman, M., *J. Physique* **36** (1975) 59.

[12] Riviere, D., Levy, Y. and Guyon, E., *J. Physique Lett.* **40** (1979) L-215.

[13] Naemura, S., *App. Phys. Lett.* **33** (1978) 1 and *J. Physique Colloq.* **40** (1979) C3-514.

[14] Scheffer, T. J. (private communication); DMOAP stands for N, N-dimethyl-N-octadecyl-3-aminopropyltrimethoxysilyl chloride.

[15] Schadt, M. and Muller, F., *IEEE Trans. Electr. Dev.* **25** (1978) 1125.

[16] Schadt, M. and Gerber, P. R., SID International Symposium Digest of Technical Papers, vol. XII, 80 (1981).

[17] Yang, K. H. and Rosenblatt, C., *Appl. Phys. Lett.* (July 1 issue, 1983).